IUST
Iran University of Science and Technology

Iranian Journal of Electrical and Electronic Engineering

Journal Homepage: ijeee.iust.ac.ir

A Dependable Protection Scheme for Electrical Vehicle Integrated Microgrid Considering Stressed Fault Scenarios and Dissimilar Fault Inceptions

Shankarshan Prasad Tiwari*(C.A.)

Abstract: In recent years, due to the widespread applications of DC power-based appliances, the researchers attention to the adoption of DC microgrids are continuously increasing. Nevertheless, protection of the DC microgrid is still a major challenge due to a number of protection issues, such as pole-to-ground and pole-to-pole faults, absence of a zero crossing signal, magnitude of the fault current during grid-connected and islanded mode, bidirectional behaviour of converters, and failure of the converters due to enormous electrical stress in the converter switches which are integrated in the microgrid. Failure of the converter switches can interrupt the charging of the electrical vehicles in the charging stations which can affect transportation facilities. In addition to the above mentioned issues protection of the DC microgrid is more challenging when fault parameters are varying due to dissimilar grounding conditions and varying operational dynamics of the renewable sources of energy. Motivated by the above challenges a support vector machine and ensemble of k-nearest neighbor based protection scheme has been proposed in this paper to accurately detect and classify faults under both of the modes of operation. Results in the section 5 indicate that performance of the protection scheme is greater as compared to other algorithms.

Keywords: DC Microgrid, Fault Detection, Support Vector Machine, Ensemble of k-Nearest Neighbor, Grid Connected and Islanded Mode

1 Introduction

THE need of the electrical power generation is rapidly growing in the modern era due to the development of electrical and electronic apparatus around the world. A number of bulk power-generating sites have been installed around the world in dissimilar locations to balance power requirement, but they are unable to fulfil the practical demand of the electrical power. The major drawbacks of such type of power generation units are the availability of the fuel throughout year, contamination of the air quality due to the continuous emission of air particles, degradation of the wildlife and human lives. Therefore, the energy scenario is rapidly shifting from traditional, non-renewable sources of energy such as coal, nuclear fuel, and petroleum products to renewable sources of energy (biomass, solar, wind, tidal, and geothermal). The microgrid is the best option to provide such demand of electrical power which is amalgamation of low-rated renewable DERs, converter loads, and energy storage devices [1–3] with some clearly defined electrical boundaries. The DC microgrid has become a proficient and reliable power system in the field of power technology. On the basis of the power output at buses, the DC microgrid can be categorized into three categories: AC, DC, and a combination of AC and DC. In the above three classes, wider acceptance of the DC microgrid in a number of applications, such as EV charging stations [4], DC-operated cars, trolly cars,

Iranian Journal of Electrical & Electronic Engineering 2024.
Paper first received 02 July 2023 and accepted 07 March 2024.
*The author is with the Department of Electrical Engineering, National Institute of Technology Raipur, Chhattisgarh, India
E-mail: shankarshan.tiwari20@gmail.com, shankarshan.tiwari@siem.org.in
* Corresponding Author: Shankarshan Prasad Tiwari.

electric savers, grinders, and LEDs, makes it more attractive and useful. In addition to the above-mentioned applications, it offers a number of advantages as compared to the traditional AC microgrid, such as flexibility, cost-effective [5] due to the smaller number of leads, free from synchronization, higher power transfer capacity [6], and fewer power conversion stages [7-8]. Nevertheless, protection of the DC microgrid is difficult due to a number of fault issues, such as pole-to-ground and pole-to-pole faults, bidirectional behaviour of converters and false tripping. In addition to the above conditions, detection of the fault under dissimilar fault conditions becomes tricky when the level of the fault current is rapidly changing from lower to higher level. Under these conditions, power supply at the consumer end can be affected due to the sudden disturbances, such as power interruptions in EV charging stations, load shutdowns in residential and commercial buildings, delays in production plants and transportation associated facilities. In the case of the EV charging stations, supply can be affected by a sudden increment in the current because huge electrical stress can damage to converter unit. In microgrids, due to the amalgamation of renewable sources, uncertain conditions cannot be avoided due to changes in the atmospheric conditions. Under such conditions, traditional protection schemes can malfunction. To propose the problems related to variation in the fault level simulation has been carried out in Fig. 1 and Fig. 2, where it is easily investigated that the level of the voltage and current is changing when a fault occurs at a given inception.

The main reason behind the variation in the fault current is changes in the touching conditions of the conductors which can be wet and dry soil, branches of the tree and hilly surfaces. A number of protection schemes have been reported by the authors regarding DC microgrid protection such as a differential protection scheme based on voltage of the reactor in [9], localize protection scheme for LVDC microgrid in [10], time varying filter based protection scheme in [11], a noble protection scheme based on bidirectional OZ circuit breaker in [12], an over current based communication assisted protection scheme [13], protection scheme based on inductance estimation [14], rate-of-rise of fault current based protection scheme in DC microgrid [15], local measurement-based protection scheme [16], a poverty severity index-based protection scheme [17],oscillation frequency component-based protection scheme [18], compensation gain and artificial line inductance based scheme in [19], EMD/HT-based local fault detection in DC microgrid in [20], identification of the impedance ground faults in the DC microgrid in [21], protection scheme for identification of the high impedance fault with inclusion of the VSC based generation in [22], after considering a communication failure a protection scheme has been proposed in [23] and a protection scheme based on solid-state circuit breaker in [24]. Nevertheless, existing schemes are not considering varying fault scenarios as well as uncertainty. The output of renewable DERs such as PV and wind can't be the same due to uncertainty in wind speed and irradiances, therefore impact of the renewable sources in the microgrid can't be ignored.

In the case of the traditional power distribution system, the development of the protection scheme was not too tedious due to the absence of such DERs, but in recent microgrid it is quite difficult. For a ring-based system, development of the protection scheme is more difficult when comparing with other types of the system (radial system). Therefore, in this work, SVM and an ensemble of kNN-based algorithms have been proposed to provide stability in the system during faulty conditions. The major contribution of the work can be summarized as follows:

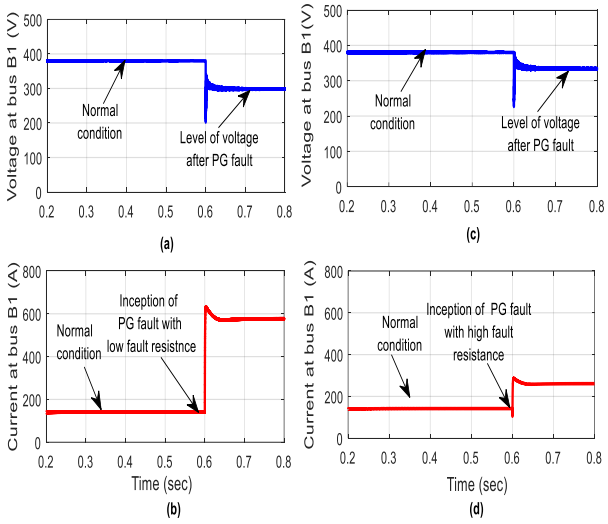

Fig. 1 (a), (b) Variation in level of voltage and current during PG fault under grid connected mode (c), (d) Variation in level of voltage and current during PG fault under grid connected mode

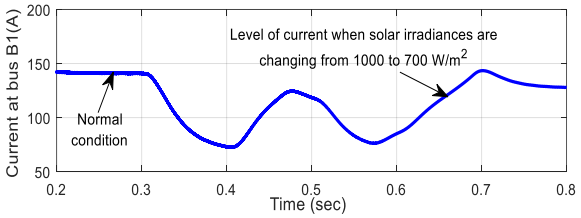

Fig. 2 Level of current after variation in the solar irradiances

- Enhancing the reliability of the system by prompt identification of faults using single bus data and avoiding additional cost of the link.

- Development of a protection scheme for mode detection in proposed EV integrated microgrid, fault detection/classification, and faulty section identification.
- Avoiding malfunctioning of relays due to high penetration of PV and wind-based DERs and validating the protection scheme through testing of the proposed modules.

The rest of the manuscript is organized as follows: In Section 2, a single-line diagram of the DC microgrid is given, while Section 3 deals with an overview of the proposed algorithm. In Section 4, the development of the protection scheme is given, while in Section 5, the performance of the protection scheme is given, followed by conclusion in Section 6.

2 Single Line Diagram of the Four Bus DC Microgrid

In this section, the layout of the proposed 380 V, DC microgrid is given. In the proposed DC microgrid system, a total of four buses have been used (Fig. 3) to amalgamate the DERs in dissimilar locations. As given in the microgrid that DERs are integrated in dissimilar locations therefore, converters are used in the microgrid model, where sources are integrated through the DC to DC and AC to DC converters. The overall length of the microgrid system is 5 kilometer and a total of four sections are used to connect the units of the DC microgrid. Apart from the above, twelve faults (F1 to F12) have also been used to observe variations in the fault current level under dissimilar operating scenarios. To connect utility grid from the rest of the microgrid an AC-to-DC bidirectional converter has been used. L is the DC load which is connected between bus -1 and bus-4. The model has been developed in the MATLAB/SIMULINK environment.

3 Overview of Proposed SVM and Ensemble of kNN Based Algorithm

3.1 Support Vector Machine (SVM)

Support vector machines, the most widely used machine learning method, are mostly used for

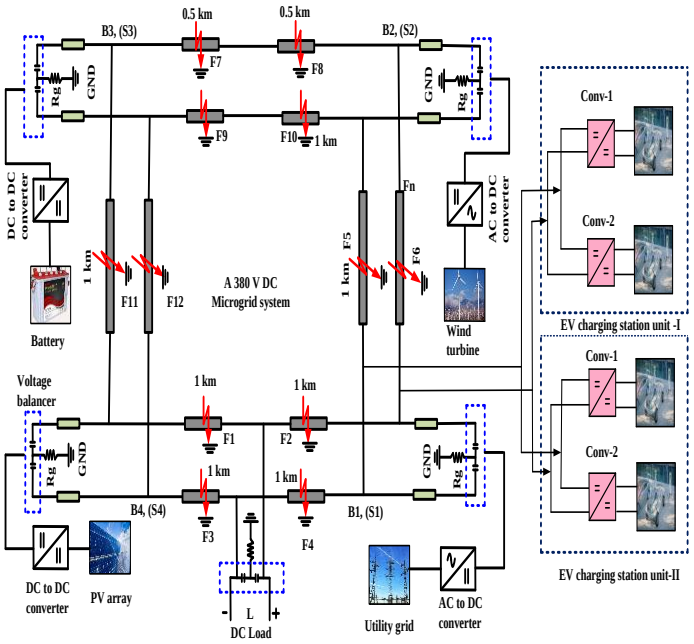

Fig. 3 Single line diagram of the test microgrid system

classification. Fig. 4 demonstrates a basic layout of the SVM where support vectors and separating hyperplane can be easily observed when using it for classification purposes. It uses the concept of pattern reorganization and it is a supervised learning-based for categorizing incoming data. A set of hyperplanes in infinite space is used in SVM to categorize the input data [25-26]. Based on an evaluation of the maximum separation between the closest and farthest data points, any class is separated. The accuracy of the system will increase if the margin between the separation points is large, since the classifier will make fewer errors.

The hyperplane equation for class separation is given by the equation below:

$$T = (ai, bi), < i < n \quad (1)$$

Where a_i and b_i shows the real vector and class of data respectively. The classes can be represented as:

$$w.x - c = 0 \quad (2)$$

In above equation w, x, and c, are the normal vector, setting point in hyperplane and bias.

The first and second classes of data can be represented by the below equations, respectively.

$$w.x - c \geq +1 \quad (3)$$

$$w.x - c \leq -1 \quad (4)$$

where, +1 and -1 indicates first and second classes, respectively. Suppose if m is the margin then separation margin is given by below equation:

$$m = \frac{2}{||w||} \quad (5)$$

For greater margin the value of the m should be increase.

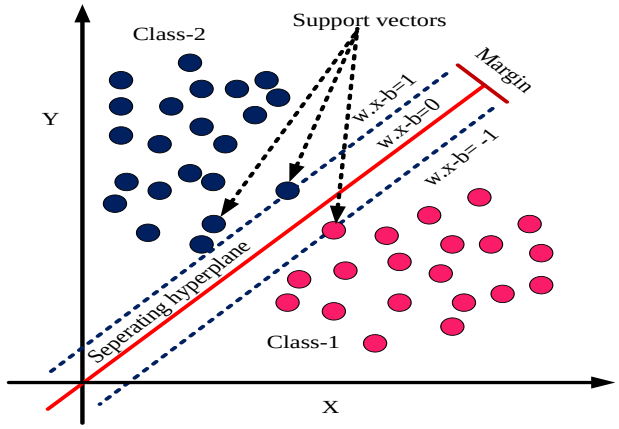

Fig. 4 Layout of the support vector machine

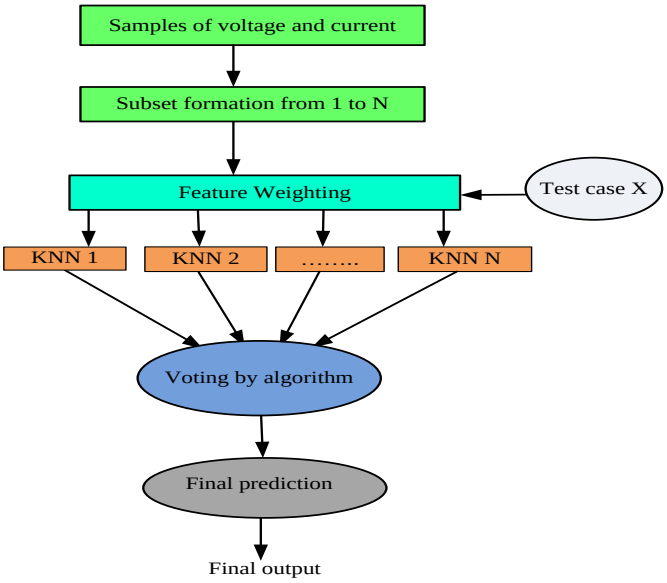

Fig. 5 Random subspace model of the proposed ensemble

3.2 Ensemble of kNN

The usefulness of an ensemble of classifiers in achieving robust performance for larger datasets has been used in the current study to construct classifier modules for DC micro-grid protection [27]. An ensemble technique eliminates any potential bias that a single classifier might have by combining multiple classifiers, or individual predictions, through a voting process to decide the final class for a given input. The random subspace technique has the capacity to learn data quickly, with the aim of protecting the power distribution network appropriately. The ensemble classifier random subspace ensemble method is depicted in Fig. 5. In below figure it is clearly demonstrated that firstly samples of the voltage and current has been used then further processed for subset formation. After feature weighting algorithm will execute in next stage for further action. The kNN is used as a base classifier in the algorithm which is used for performing assigned tasks.

$$\sum_{i=1}^{T} W_i d_{k,m} = max_{m=1}^{C} \sum_{k=1}^{T} W_i d_{k,m} \qquad (6)$$

where T is classifier numbers, c is the class and $d_{k,m}$indicates output.

4. Development of the Protection Scheme (Layout of the Protection Scheme)

A protection scheme plays an important role in any type of power distribution system to increase resiliency under sudden variations in the system. It helps in the prompt restoration of the system by reducing the probability of failure in the power system. Therefore, in this section, the development of the protection scheme has been proposed in Fig. 6 to identify mode of operation or mode detection, fault detection/classification and faulty section identification under grid-connected and islanded modes of operation. To design an efficient protection scheme, hybrid modules have been used, which are SVM and ENSkNN. A total of five modules have been used, where SVM is used for mode identification, i.e., grid-connected or islanded, while later modules are used for fault detection/classification (ENSkNN-1 and ENSkNN-3) and faulty section identification (ENSkNN-2 and ENSkNN-4) under both of the modes. The sequence of the protection scheme can be understood as follows: Firstly, voltage and current signals are retrieved from a simulation of the dissimilar operating scenarios of the proposed microgrid and then fed into the first module, i.e., SVM, for identification of the mode of operation. Once the mode has been identified, the algorithm automatically triggers the next-stage modules for the-

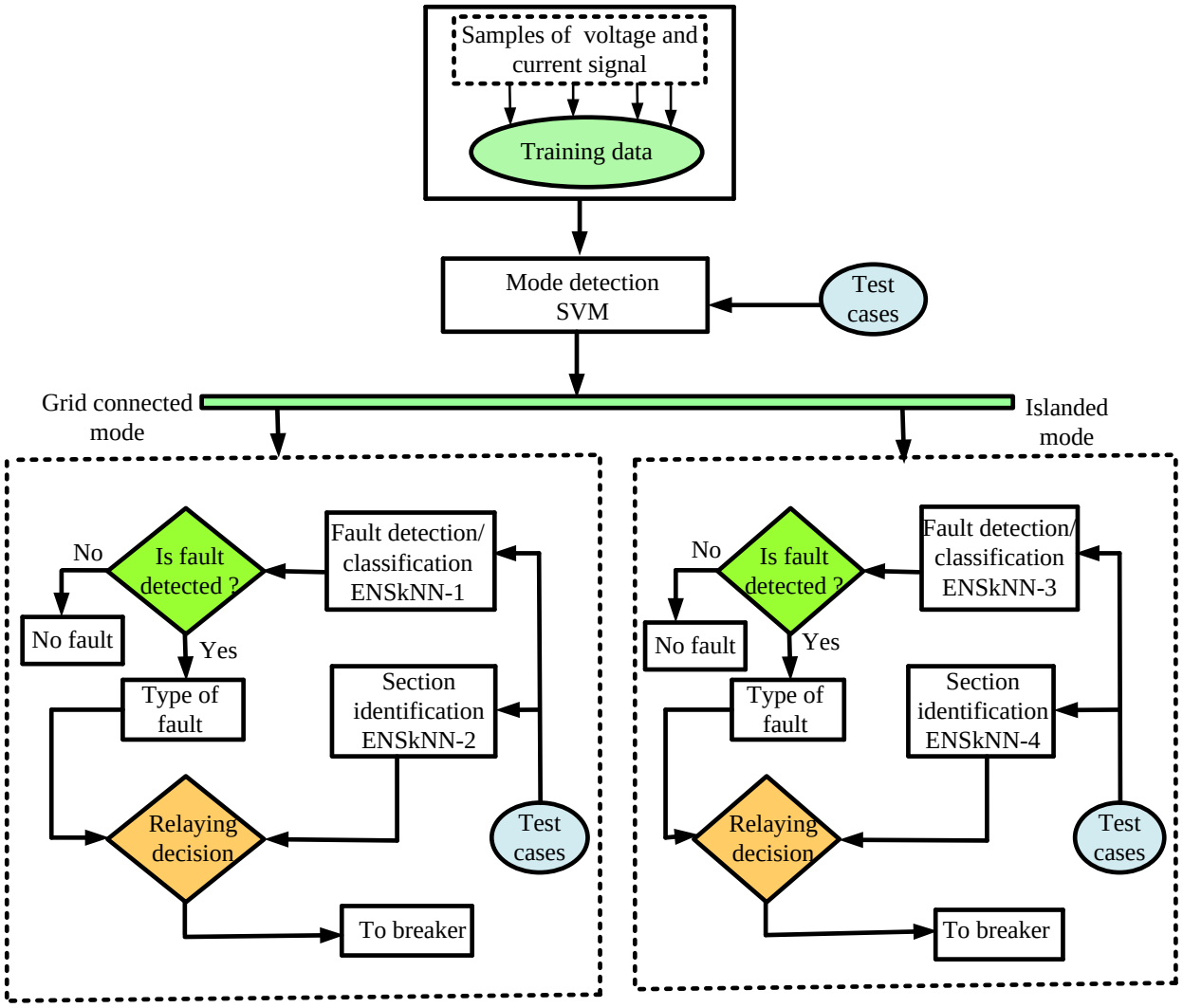

Fig. 6 Schematic diagram of the protection scheme

assigned tasks of fault detection/classification and faulty section identification. After successful identification of the fault and faulty section, the relay will issue a trip signal to operate the circuit breaker, which will disconnect the faulty section from the healthy section.

5. Performance Analysis

The performance of the protection scheme has been evaluated in this section to investigate the invulnerability of the protection scheme in both of the modes. A number of parameters, such as length of the fault, fault inception, fault resistance, and faulty sections, have been considered during the analysis of the protection scheme. A total of 18000 cases under both modes have been-generated through the proposed test microgrid model (Table 1). For data generation, two categories of faults have been used, where a variety of parameters have been used for the PG fault. For the PP fault, a total of 1200 cases have been generated through one value of the fault resistance and the same combination of the parameters. In addition to the above fault scenarios, 100 no-fault cases have also been used that are simulated under healthy conditions. For training and testing of the modules, the overall datasets have been divided in the ratio of 70% and 30%. After testing the modules, the performance of the protection scheme has been validated in various subsections. Table 1 shows the complete details of the data generation for training and testing of the modules.

Table 1 Generation of the data for training and testing of the modules

Parameters during training of classifier	Specification of fault parameters during training	Total cases	Total training cases	Total testing cases
Types of fault (PG and PP)	2	PG fault cases=16800 PP fault cases=1200 16800+1200= 18000+100=1 8100	12600+7 0=12670	5470+30= 5430
Fault resistance (5Ω-100Ω and 0.3Ω)	15			
Length of fault (5 cases in each section)	20			
Variation in Is and Ws (10 cases for each)	20			
Inception of fault (0.5,0.6 and 0.7)	3			
No fault cases	100			

Table 2 Performance of the mode detection module

Names of the techniques	Operating modes		
	Grid connected (%)	Islanded (%)	Overall accuracy (%)
SVM	100	99.21	99.60
DT	97.84	98.43	98.13
LDA	96.55	96.88	96.71

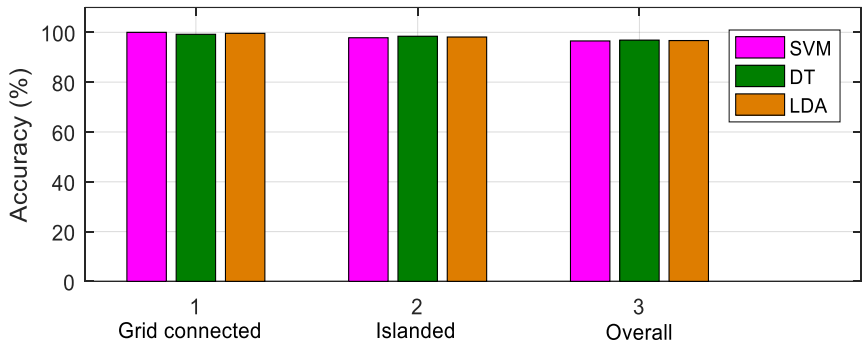

Fig. 7 Comparative analysis of percentage accuracy (mode detection module)

5.1 Mode Detection (SVM Module)

The magnitude of the fault current can change in the islanded mode of operation due to the dissimilar contribution of the fault current. This condition demands a protection scheme that can easily discriminate between modes of operating modes, i.e., grid-connected or islanded for both types (PG and PP) of the fault. Higher accuracy is necessary for smooth operation of the mode identification module therefore, in this subsection, the performance of the mode detection module has been evaluated under grid-connected and islanded modes of operation. In the proposed protection scheme, a SVM-based module has been used for mode detection due to its significant properties for two-class classification. To validate the mode detector module a total of 3640 test cases under both modes have been used and their outcomes after successful testing are proposed in Table 2. To compare the efficacy of the proposed module when identifying operating mode, two other machine learning-based algorithms have also been considered which are tested on the same testing datasets. The results in the below table indicate that the protection scheme is effectively performing the task of mode identification. A bar graph in Fig. 7 has been plotted to show the differences in the percentage accuracy of the mode detector module.

Table 3 Performance comparison of proposed fault detector classifier in terms of reliability indices

Name of algorithms	Mode of operation					
	Grid connected			Islanded		
	Dependability (%)	Security (%)	Overall accuracy (%)	Dependability (%)	Security (%)	Overall accuracy (%)
ENSkNN	99.56	99.61	99.58	98.35	98.47	98.41
DT	96.57	96.45	96.51	95.85	95.62	95.73
LDA	95.74	93.86	94.80	93.27	92.11	92.69

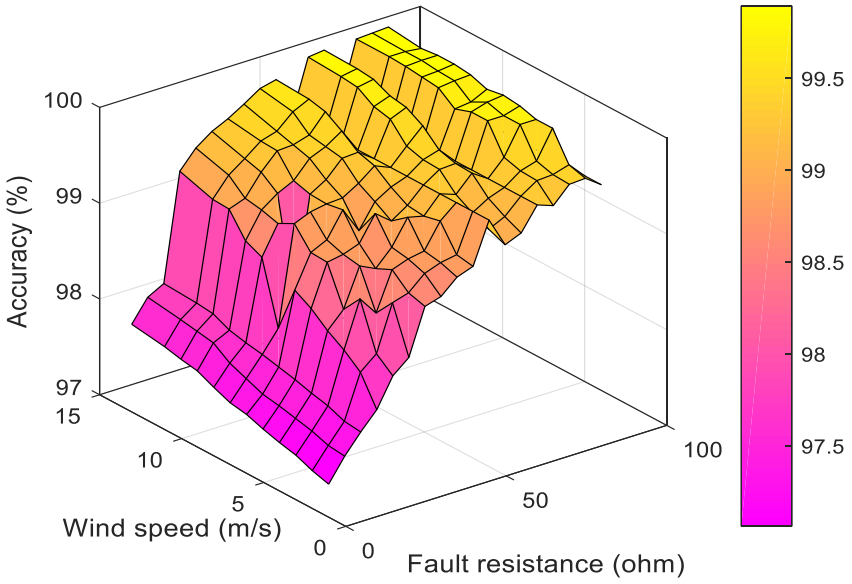

Fig. 8 3D presentation of the fault detector/classifier module (grid connected mode)

5.2 Fault Detection/Classification (ENSkNN-1 and ENSkNN-3)

To restore the power distribution network, prompt identification of faulty conditions is necessary to reduce any probability of power blackouts in the connected areas. Therefore, in this subsection, the accuracy of the fault detector/classifier modules has been evaluated under grid-connected and islanded modes of operation. For the investigation of the modules, statistical analysis has been carried out through reliability indices, which are dependability and security. Dependability helps in the identification of the actual predicted fault cases, while security confirms the actual predicted no-fault cases. A total of 1260 test cases, including 30 no-fault cases have been used for the testing of the modules. The test results in Table 3 indicate that the proposed fault detection modules are efficiently performing the assigned tasks under both of the modes. Further, the fault detection accuracy of the proposed fault detection module has been compared with DT and LDA-based classifiers. To clearly demonstrate the variation in fault detection/classification accuracy, a 3D plot has been considered in Fig. 8, where it is observed that the accuracy of the proposed protection scheme for fault detection/classification is higher and it is above 97.50%.

5.2.1 Sensitivity Analysis

Sensitivity analysis has been carried out in this subsection to investigate truly detected fault cases for grid connected and islanded mode. Sensitivity analysis

Table 4 Performance during sensitivity analysis

Operating modes	Cases given (TP)	Cases predicted (TP+FN)	Overall percentage
Grid connected	480	476	99.16
	540	535	99.07
Islanded	480	472	98.33
	540	532	98.51

Table 5 Performance of the section identifier modules

Mode of operation	Section	No of test cases	Types of fault	ENSkNN (%)	DT (%)	LDA (%)
Grid connected mode	S1	340	PG	98.46	96.89	94.64
	S2	260	PP	98.55	96.63	93.56
	S3	280	PG	98.74	96.17	94.89
	S4	160	PP	99.12	97.94	94.68
	Overall accuracy (%)			98.71	96.90	94.44
Islanded mode	S1	540	PG	98.06	95.83	93.26
	S2	640	PP	97.34	95.46	93.15
	S3	380	PG	97.47	95.73	94.12
	S4	460	PP	96.85	96.86	93.72
	Overall accuracy (%)			97.43	95.97	93.56

helps in the analysis of the true positive and false positive cases (Eq.7) that have been identified. Table 4 shows indicate complete details about the sensitivity of the scheme under different fault scenarios. In the below table, it is observed that the achieved values are higher, which shows the robustness of the protection scheme.

$$\frac{TP}{TP+FN} \quad (7)$$

5.3 Section Identification (ENSkNN-2 and ENSkNN-4)

Prompt identification of the faulty section helps in the quick restoration of the power to consumer, therefore in this subsection, the performance of the section identifier module has been investigated under grid-connected and islanded modes of operation. To validate the proposed section identifiers, a total of 2080 test cases have been used under dissimilar faulty conditions where pole-to-ground and pole-to-pole faults have been considered for analysis of the section identifier modules. The result in Table 5 reveals that the protection scheme is robust and accurate when identifying faulty sections in both of the operating modes. The overall percentage accuracy found during section identification is 98.71% and 97.43% under grid-connected and islanded mode for the proposed protection scheme, while it is less for DT and kNN-based section identifier modules.

5.4 Performance of the Protection Scheme under Dissimilar Operating Scenarios

In this sub-section protection scheme has been evaluated under dissimilar fault inceptions and other operating parameters as dealt in Table 6. The range of the fault resistance during the validation of the scheme is taken between 60 and 100 ohm for a pole-to-ground fault, while it is less for a pole-to-pole fault. In addition to the mentioned conditions, wind speed is also taken between 4 m/s and 15 m/s, while length is between 0.5 km and 4 km. The results in Table 6 indicate that the protection scheme is efficient and reliable when parameters are changing. To depict the generation of the trip signals, Fig. 9 has been used, where dissimilar fault inceptions are given in (a), (b), and (c). Responses in the below figure show that protection scheme is rapidly identifying faults.

Table 6 Performance of the scheme under dissimilar fault inceptions and length of the fault

Types of mode	Type of fault	Fault resistance (Ω)	Fault inception	Length of the fault (km)	Wind speed (m/s)	Protection scheme response	Relay trip time(ms)
Grid connected	PG	60	0.6	0.5	15	PG	2.6
	PG	85	0.5	1	12	PG	2.9
	PG	100	0.7	2.5	10	PG	3.2
	PP	0.3	0.6	3	6	PP	2.5
	PP	0.3	0.5	3.5	4	PP	2.4
	PP	0.3	0.7	4	12	PP	2.3
Islanded	PG	60	0.6	0.5	15	PG	3.2
	PG	85	0.5	1	12	PG	3.4
	PG	100	0.7	2.5	10	PG	3.4
	PP	0.3	0.6	3	6	PP	2.7
	PP	0.3	0.5	3.5	4	PP	2.8
	PP	0.3	0.7	4	12	PP	2.6

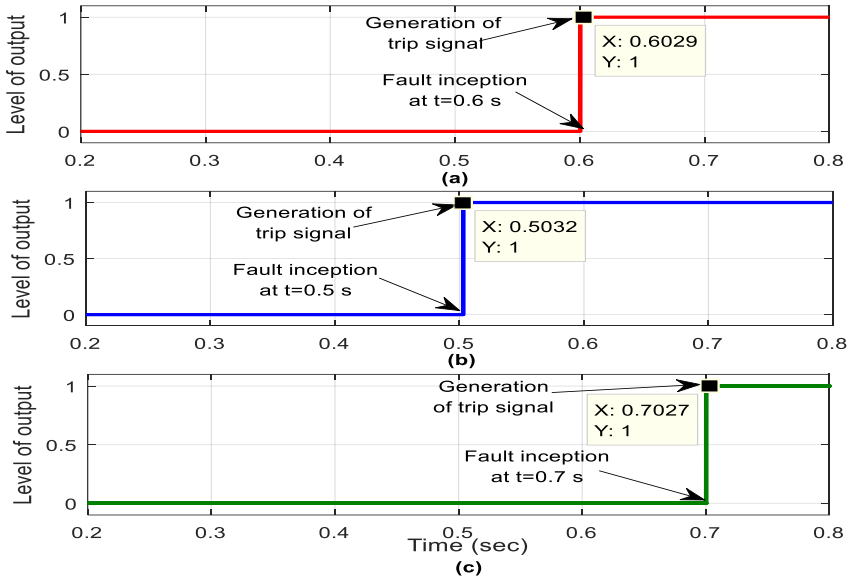

Fig. 9 Generation of trip signal under dissimilar fault inceptions

5.5 Performance of the Protection Scheme under Dissimilar Solar Irradiances and Fault

Performance of the protection scheme has been validated in this subsection to investigate accuracy under changes in solar irradiances and fault resistances. The range of the fault resistance is taken between 5 and 100 ohm, while solar irradiances are taken between 400 W/m^2 and 1000 W/m^2 under grid-connected and islanded modes of operation. The results in Table 7 indicate that the protection scheme is accurately detecting the fault.

5.6 Response of the scheme in grid connected and islanded mode under load variations

Rapid variations in the load can cause unwanted tripping (false tripping), which can lead to the maloperation of the traditional relays. Therefore, in this subsection, the response of the protection scheme has been validated under varying load conditions and dissimilar types of faults. The parameters and range of the variations are completely given in Table 8, where values can be easily observed.

Table 7 Performance during load variation in solar irradiances and fault

Operating modes	Type of fault	Fault resistance (Ω)	Dissimilar solar irradiances (W/m^2)	Accuracy (%)
Grid connected	PG	5	400	98.56
	PG	8	700	98.67
	PG	10	100	98.86
Islanded	PG	50	500	99.16
	PG	80	700	98.84
	PG	100	900	98.66
Grid connected	PP	0.3	400	98.45
	PP	0.3	700	98.44
	PP	0.3	100	99.24
Islanded	PP	0.3	500	98.26
	PP	0.3	700	99.11
	PP	0.3	900	99.26

Table 8 Response of the scheme for change in load conditions and variations in the wind seed and solar irradiances

Operating modes	Change in load (linear load) %	Fault type	Change in wind speed and solar irradiances	Section	Response of the protection scheme	Status of the EV
Grid connected	± 20	PG	8 m/s, 200 W/m^2	S1	PG	Connected
	±30	PG	10 m/s, 300 W/m^2	S3	PG	
	±40	PG	12 m/s, 500 W/m^2	S4	PG	
	±50	PG	15 m/s, 700 W/m^2	S3	PG	
Islanded	± 20	PP	8 m/s, 200 W/m^2	S1	PP	
	±30	PP	10 m/s, 300 W/m^2	S3	PP	
	±40	PP	12 m/s, 500 W/m^2	S4	PP	
	±50	PP	15 m/s, 700 W/m^2	S3	PP	

Table 9 Comparison of the protection scheme with other protection scheme of the microgrid

Parameters of comparison	DC Microgrid existing protection schemes			
	[11]	[13]	[14]	Proposed scheme
Input features	Current	Voltage	Current	Voltage and current
Parameters used during analysis	Fault-resistance and location	Fault-resistance	Fault- resistance	Fault- Resistance, length of fault, location of fault
Tasks	Fault-detection	Detection task only	Fault-detection and classification	Fault detection and classification, location estimation
Communication link	Yes (required)	Yes (required)	Yes (required)	No (not required)
Total number of test cases	Not-considered	Not-considered	Not-considered	5430
Variation in wind speed in protection scheme	Not	Not	Not	Yes (a number of cases have been considered)

In addition to the above, further resiliency of the protection scheme has been validated, with changes in wind speed and solar irradiances have also been considered in both operating modes. All the cases have

been validated when EV charging stations are connected to the microgrid. The details in the below table indicate that the protection scheme is accurately operating under diverse operating conditions.

6. Conclusion

In the proposed work, a protection scheme based on SVM and ENSkNN has been proposed for electrical vehicle integrated microgrid to perform the tasks of mode detection, fault detection classification, and section identification under grid-connected and islanded modes of operation. After validation of the modules, achieve accuracy was 100% and 99.21% for mode identification modules, 99.58% and 98.41% for fault detection and classification modules. In protection scheme voltage and signals were used for training and testing of the modules. A number of fault parameters were used for analysis of the protection scheme for validation of the protection scheme. In last subsection performance of the protection scheme has been compared with the exiting protection schemes of the DC microgrids. The results in the section 5 indicate that the protection scheme is efficiently performing the tasks of the mode detection, fault detection/classification and faulty section identification. The proposed work can be extended with huge penetration of renewable sources as well as multiple charging stations that are integrated into microgrids with the help of converters.

Acronyms

PG- Pole to ground; PP- Pole to pole; PV- Photovoltaic; UG- Utility grid; PCC- Point of common coupling kNN-k nearest neighbour SVM- Support vector machine; DT-Decision tree; LDA- Linear discriminate analysis; LEDs- Lighting emitting diodes; DERs- Distributed energy resources; LVDC- Low voltage DC microgrid

Symbols

ms-millisecond, km-Kilometer, Ω-ohm, kW- Kilowatt, W/m2-Watt per meter square,%-Percentage, m/s- Meter per second, L – DC Load, F1 to F12- Fault

Intellectual Property

The author confirm that he has given due consideration to the protection of intellectual property associated with this work and that there are no impediments to publication, including the timing to publication, with respect to intellectual property

Funding

No funding was received for this work.

CRediT Authorship Contribution Statement

Shankarshan Prasad Tiwari: Data curation, Conceptualization, Methodology, Software, Formal analysis, Original draft writing, Review and editing.

Declaration of Competing Interest

The author hereby confirms that the submitted manuscript is an original work and has not been published so far, is not under consideration for publication by any other journal and will not be submitted to any other journal until the decision will be made by this journal. The author has approved the manuscript and agrees with its submission to “Iranian Journal of Electrical and Electronic Engineering

Reference

[1] M. Uddin, H. Mo, D. Dong, S. Elsawah, J. Zhu, and J.M. Guerrero, "Microgrids: A review, outstanding issues and future trends," *Energy Strategy Reviews*, Vol. 49: pp.101127, 2023

[2] G.P. Santos, A. Tsutsumi, and J.C.M. Vieira, "Enhanced voltage relay for AC microgrid protection," *Electric Power Systems Research*, Vol. 220, pp.109310, 2023

[3] S.P. Tiwari, "Fault detection in ring based smart LVDC microgrid using ensemble of decision tree," Iranian Journal of Electrical and Electronic Engineering Vol. 18, No. 4, pp.2600-2600, 2022

[4] N. Poursafar, S. Taghizadeh, M.J. Hossain, and F. Blaabjerg "An enhanced control strategy for an ultra-fast EV charging station in a DC microgrid," *International Journal of Electrical Power & Energy Systems*, Vol. 146, pp.108727, 2023

[5] N. Bayati, H.R. Baghaee, A. Hajizadeh, M. Soltani, and Z. Lin, “Mathematical morphology-based local fault detection in DC Microgrid clusters,” *Electric Power System Research*, Vol.192, pp.106981, 2021

[6] Z. Zhang, C. Qing, X. Ranran, and S. Kongming, “The fault analysis of PV cable fault in DC microgrids,” *IEEE Trans. on Energy Conversion*, Vol. 34, No.1, pp.486-496.2018.

[7] J.C. Ciezki, and R.W. Ashton,“Selection and stability issues associated with a navy shipboard DC zonal electric distribution system,” IEEE Transactions on Power Delivery, Vol. 15, No.2, pp.665-669, 2000.

[8] OVG Swathika, and S. Hemamalini, “Prims-Aided Dijkstra algorithm for adaptive protection in microgrids,” *IEEE Journal of Emerging and Selected Topics in Power Electronics*, Vol.4, No.4, pp.1279-1286, 2016

[9] S. Sharma, and M. Tripathy, "Differential reactor voltage based fault detection and classification for smart DC microgrid," *IEEE Transactions on*

Industrial Informatics, Vol. 19, No. 12, pp. 11730-11741, 2023

[10] P. Chauhan, C.P. Gupta, and M. Tripathy. "High speed fault detection and localization scheme for low voltage DC microgrid," *International Journal of Electrical Power & Energy Systems*, Vol. 146, pp.108712, 2023

[11] S. Sarangi, C. Biswal, B. K. Sahu, I.S. Samanta, and P. K. Rout, "Fault detection technique using time-varying filter-EMD and differential-CUSUM for LVDC microgrid system," *Electric Power Systems Research*, Vol. 219, pp.109254, 2023

[12] Z. Zhou, J. Jiang, S. Ye, D. Yang and J. Jiang,"Novel bidirectional O-Z-source circuit breaker for DC microgrid protection," IEEE Transactions on Power Electronics, Vol. 36, no. 2, pp. 1602-1613, 2021

[13] A. Shabani and K. Mazlumi,"Evaluation of a communication-assisted overcurrent protection scheme for photovoltaic-based DC microgrid," *IEEE Transactions on Smart Grid*, Vol. 11, No. 1, pp. 429-439, 2020

[14] M. Shamsoddini, B. Vahidi, R. Razani, and Y. A.R.I. Mohamed, "A novel protection scheme for low voltage DC microgrid using inductance estimation," *International Journal of Electrical Power & Energy Systems*, Vol.120, pp.105992, 2020

[15] P. Chauhan, C.P. Gupta, and M. Tripathy, "A novel adaptive protection technique based on rate-of-rise of fault current in DC microgrid," *Electric Power Systems Research*, Vol. 207, pp. 107832, 2022

[16] M.R.K. Rachi, M.A. Khan and I. Husain, "Local measurement-based protection coordination system for a standalone DC microgrid." *IEEE Transactions on Industry Applications*, Vol. 57, No. 5, pp. 5332-5344, 2021

[17] M. Salehi, S. A. Taher, I. Sadeghkhani and M. Shahidehpour, "A poverty severity index-based protection strategy for ring-bus low-voltage DC microgrids," IEEE *Transactions on Smart Grid*, Vol. 10, No. 6, pp. 6860-6869, Nov. 2019,

[18] S. A. Wakode, M. S. Ballal, A. A. Sheikh and R. R. Deshmukh, "Oscillation frequency component-based protection scheme for DC microgrid," IEEE *Transactions on Industry Applications*, Vol. 57, No. 6, pp. 5747-5757, 2021

[19] M. Shamsoddini, B. Vahidi, R. Razani, and H. Nafisi, "Extending protection selectivity in low voltage DC microgrids using compensation gain and artificial line inductance," Electric Power Systems Research, Vol.188, pp.106530, 2020

[20] N. Bayati, H.R. Baghaee, M. Savaghebi, A. Hajizadeh, M. Soltani, and Z. Lin. "EMD/HT-based local fault detection in DC microgrid clusters." *IET Smart Grid*, Vol.5, No. 3, pp.177-188, 2022.

[21] Wang, Xiaodong, Ruojin Wang, Yingming Liu, and Xing Gao, "Impedance ground faults detection and classification method for DC microgrid," *Journal of Electrical Engineering & Technology*, pp.1-13, 2023

[22] V. F. Couto and M. Moreto, "High impedance fault detection on microgrids considering the impact of VSC based generation," *IEEE Access*, Vol. 11, pp. 89550-89560, 2023

[23] W. Zhang, H. Zhang and N. Zhi, "A novel protection strategy for DC microgrid considering communication failure," *Energy Reports*, Vol.9, pp.2035-2044, 2023

[24] X. Xu, J. Ye, Y. Wang, X. Xu, Z. Lai and X. Wei, "Design of a reliable bidirectional solid-state circuit breaker for DC microgrids," IEEE *Transactions on Power Electronics*, vol. 37, no. 6, pp. 7200-7208, June 2022

[25] J.M. Johnson, and Anamika Yadav, "Complete protection scheme for fault detection, classification and location estimation in HVDC transmission lines using support vector machines." *IET Science, Measurement & Technology*, Vol.11, No. 3, 2017, pp.279-287.

[26] J Wang, D Gao, S Zhu, S Wang, H Liu. "Fault diagnosis method of photovoltaic array based on support vector machine." Energy sources, part a: recovery, utilization, and environmental effects, Vol.45, No. 2, pp.5380-5395.

[27] S.P. Tiwari, "An efficient protection scheme for wind integrated microgrid considering dissimilar AC Faults and varying fault resistance," *Iranian Journal of Electrical & Electronic Engineering*, Vol.19, No.3. pp. 152-164, 2023

Shankarshan Prasad Tiwari received the Ph.D. Degree in Electrical Engineering from National Institute of Technology (NIT) Raipur, Chhattisgarh, India in 2024, Master of Business Administration in Operations Management from Sikkim Manipal University in 2017, Master Degree in Power System from Rajiv Gandhi Proudyogiki Vishwavidyalaya, Bhopal, Madhya Pradesh, India, in 2014, Bachelor's Degree in Electrical and Electronics Engineering from Rajiv Gandhi Proudyogiki Vishwavidyalaya in 2010, respectively. He is currently working as an Assistant Professor in the Department of Electrical Engineering, Sandip Institute of Engineering and Management, Nashik, Maharashtra, India, since August, 2024. His research areas include power system protection, energy conservation management and artificial intelligence.